

Thermal studies on electrodeposited black oxide coating on magnesium alloys

A.K. Sharma^{a,*}, R. Uma Rani^a, S.M. Mayanna^b

^aThermal Systems Group, ISRO Satellite Centre, Bangalore 560 017, India

^bDepartment of Chemistry, Central College Campus, Bangalore University, Bangalore 560 001, India

Received 11 October 2000; received in revised form 17 April 2001; accepted 19 April 2001

Abstract

Thermal behavior of black anodic coatings on magnesium alloy, AZ31B and magnesium lithium alloy, MLA 9 has been investigated. The chemical nature of coating is characterized by infrared spectral studies. The thermoanalytical investigations have been carried out using thermogravimetry (TG), derivative thermogravimetry (DTG), and differential scanning calorimetry (DSC). The decomposition proceeds through three steps viz., dehydration, decomposition of chromium hydroxide and sulphate and decomposition of magnesium chromate to oxide. Measurement of hemispherical emittance of coatings versus temperature was investigated using calorimetric methods. The studies revealed that the thermal emittance of coatings increases with temperature. © 2001 Elsevier Science B.V. All rights reserved.

Keywords: Thermoanalytical behavior; Anodic coatings; Magnesium alloys; Thermal emittance; Space applications

1. Introduction

Magnesium is characterized by low density and high reactivity. Magnesium alloys are the lowest density engineering alloys used in a wide range of applications. These alloys are the promising candidates in aerospace and allied fields primarily to save the fuel cost. Attempts have been made for addition of various alloying elements to magnesium so as to produce alloys of high strength, high creep resistance and low density.

Magnesium–lithium alloys are the lightest structural metallic alloys known today. Addition of lithium with a relative density of 0.53, in magnesium reduces

the density of alloy significantly. Furthermore, addition of ~11% lithium converts hexagonal close packed structure of pure magnesium to the body centered cubic lattice, markedly improving formability of the alloy [1]. The binary magnesium–lithium alloys, though light and ductile are not strong. Addition of aluminum results in considerable improvement in strength, primarily due to the formation of Mg Li₂ Al metastable phase [2–4]. Magnesium–lithium alloy, MLA 9, containing 11–13% Li, 1.25–1.75% Al, and balanced Mg wt.%, is developed at Defence Metallurgical Research Laboratory (DMRL), Hyderabad, India. These alloys are 25% lighter than conventional magnesium alloys (density ~1.35 g/cm³) resulting into a considerable weight saving.

Chemical conversion coatings, viz, anodizing, chromating, etc. are often employed as an ideal means of improving one or more surface properties, chemical, mechanical, electrical or optical. These are used to

* Corresponding author. Tel.: +91-80-508-3106;
fax: +91-80-508-3203.
E-mail address: aks@isac.ernet.in (A.K. Sharma).

prevent atmospheric corrosion, to increase microhardness and reducing friction on sliding surfaces; to provide better adhesion for paints, lubricants and adhesives; to impart thermal/electrical resistance; as a solid film lubricant to prevent cold welding in space conditions and to provide adequate optical surface for thermal control applications [5].

The black anodic coatings on magnesium alloys have been developed for thermal control of spacecraft and related applications. These coatings are used on the electronic housing of spacecraft to improve radiative coupling. In spacecraft some of the electronic packages, which are in operation, generate enormous heat while others, which are not in operation, face the cold deep space. This generates a high degree of temperature gradient across the internal packages of spacecraft. The flat absorber black anodic coating with high absorptance and thermal emittance helps in minimizing temperature gradient across the packages by improving their heat radiation characteristics as per the following equation [6].

$$SA_P\alpha = \sigma\epsilon AT^4$$

or

$$T = \left[\frac{SA_P\alpha}{\sigma A\epsilon} \right]^{1/4}$$

where S is the solar constant (mean value 1353 W/m^2); A_P the projected surface area of the spacecraft (m^2) perpendicular to the sun rays; α the solar absorptance of the projected area; σ the Stefan–Boltzman constant ($5.67 \times 10^{-12} \text{ W/cm}^2 \text{ K}^4$); A the total surface area of the spacecraft (m^2); ϵ the infrared emittance of the surface of exposed area; and T is the absolute temperature of the spacecraft.

As S , A_P , σ , and A are constants in this relationship, it clearly shows that the temperature of any given area of spacecraft is directly controlled by the α/ϵ ratio. Here, the term ‘absorptance’ refers to all solar radiation (X-ray, ultraviolet, visible, infrared, radio frequency, etc.), whereas the term ‘emittance’ is restricted to infrared range because thermal radiations occur mainly in the infrared region.

The coatings used in space technology require higher standards and better control than used for ground applications since space conditions are very severe and on-orbit spacecraft is not approachable for repair.

2. Experimental

2.1. Anodizing process

Galvanic black anodizing on magnesium alloy, AZ31B (Al 3.0%, Zn 2.0%, balance Mg wt.%) and magnesium–lithium alloy, MLA 9 (Li 11.9%, Al 1.5%, balance Mg wt.%) was carried out by the methods described in our previous publications [7,8]. A brief description of these procedures is given below.

2.2. A. Magnesium alloy, AZ31B

1. Ultrasonic solvent degreasing in isopropanol for 5–10 min.
2. Alkaline cleaning for 5–10 min in a solution containing 50 g/dm^3 sodium hydroxide and 10 g/dm^3 trisodium orthophosphate, operating at $60 \pm 5^\circ\text{C}$. Water rinse.
3. Acid pickling in 180 g/dm^3 chromium trioxide, 40 g/dm^3 ferric nitrate and 3.75 g/dm^3 potassium fluoride for 2 min. Water rinse.
4. Black anodizing in a solution formulated and operated as follows: Potassium dichromate, 25 g/dm^3 ; ammonium sulfate, 25 g/dm^3 ; pH 5.8; temperature, $25 \pm 2^\circ\text{C}$; cathode, stainless steel anodizing tank; anode to cathode ratio, 1:10; anodizing time, 30 min, for the standard coating thickness of 5–8 μm . Water rinse.
5. Heat treatment at 70°C for 2 h.

2.3. B. Magnesium–lithium alloy, MLA 9

1. Step 1 and 2 are same as described for magnesium alloy, AZ31B.
2. Acid pickling in 500 g/dm^3 chromium trioxide, 1 g/dm^3 ferric nitrate and $0.5\text{--}1 \text{ g/dm}^3$ potassium fluoride for 3–5 min. Water rinse.
3. Fluoride activation by dipping the specimen in hydrofluoric acid (40%) 50 ml/dm^3 for 10 min, followed by water rinsing.
4. Black anodizing in a solution composed and operated as follows: Potassium dichromate, 25 g/dm^3 ; ammonium sulfate, 25 g/dm^3 ; pH 5.5; temperature, $25 \pm 2^\circ\text{C}$; cathode, stainless steel anodizing tank; anode to cathode ratio, 1:10; anodizing time, 60 min; for the standard coating thickness of 14 to 18 μm . Water rinse.

5. Heat treatment at 70°C for 2 h.

Isolation of Black Anodic Coatings from the substrate for chemical and thermoanalytical analysis was carried out by gently scraping the film from the substrate using a sharp scalpel. While scraping the film care was taken that no substrate material should get scraped along with the coating.

2.4. Measurement techniques

The thickness of the anodic coating was measured using Isoscope MP 2B-T3 3B, Helmut Fischer (Germany), coating thickness tester. This instrument works on the eddy current principle and is used to measure the thickness of non-conductive coatings on a conductive substrate.

The chemical nature of coating was determined by using infrared spectroscopy. IR spectra were recorded on FTIR Spectrometer (Nicolet Model IMPACT 400 D) using KBr pellets in the wave number region of 4000–400 cm^{-1} .

The thermal stability of the anodic coating was investigated by using Dupont 951 thermogravimetric analyzer to record thermogravimetric (TG) and derivative thermogravimetry (DTG) curves and Dupont 910 differential scanning calorimetry (DSC) systems to record DSC curves. The thermoanalytical curves were recorded in argon atmosphere with a gas flow rate of 40 cm^3/s and a sample heating rate of 10°C/min. TG and DTG curves were recorded for 19.4 mg samples simultaneously up to 1000°C. DSC data for 15.9 mg samples were limited to a temperature of 500°C, due to limited temperature capability of the instrument.

3. Results and discussion

3.1. Infrared spectra

The assignment of IR bands has been made on the basis of published data [9–11]. The spectra of galvanic black anodic film on magnesium alloys, AZ31B and magnesium–lithium, MLA 9 are shown in Figs. 1 and 2. Strong bands associated with OH stretching vibrations of water and hydroxyl groups occur between 3200 and 3700 cm^{-1} . Water of hydration is easily

distinguished from hydroxyl groups by the presence of H–O–H bending motion, which produces a medium band in the region 1600–1650 cm^{-1} [9]. The appearance of IR absorption bands in Figs. 1 and 2 at $\sim 3435 \text{ cm}^{-1}$ are associated with OH stretching vibrations of water of hydration. The bands at 1631 cm^{-1} in Fig. 1 and 1646 cm^{-1} in Fig. 2 show the H–O–H bending motion, which confirms the presence of chromium hydroxide.

Absorption bands at $\sim 1100 \text{ cm}^{-1}$ accompanied by a considerably weaker band at $\sim 670 \text{ cm}^{-1}$ are associated with chromium sulphate [10]. The doublet occurred at 917 and 802 in Fig. 1 and the single peak at 870 cm^{-1} appeared in Fig. 2 reveal the presence of magnesium chromate [11].

The bands at lower frequencies ~ 530 , $\sim 470 \text{ cm}^{-1}$ are assigned to the stretching frequencies of M–O bonds, indicating the presence of chromium and magnesium oxides.

3.2. Hemispherical emittance

Measurements of total hemispherical emittance have been made using calorimetric method [12]. This consists of measurement of the power-input parameters and temperatures of sample and the shroud. Using these data, emittance of the black anodized surface under steady state conditions were calculated using following energy balance equation

$$\varepsilon = \frac{P}{\sigma A(T_S^4 - T_0^4)}$$

where ε is the total hemispherical emittance, P the power, Heat input to the sample (watts), σ the Stefan–Boltzmann constant ($5.67 \times 10^{-12} \text{ W/cm}^2 \text{ K}^4$), A the area of the sample (cm^2), T_S the temperature of sample (K) and T_0 is the temperature of shroud (K).

The measurements were made in a stainless steel double walled test chamber. The inner wall (shroud) is isolated from the outer wall with the Teflon spacers. The inside wall of the chamber that receives the radiation from test specimen is coated with black paint for maximizing the thermal coupling. This chamber is connected to a vacuum system to maintain the pressure inside the chamber at the level of 76×10^{-7} mbar. The measurements were carried out on a specially designed cup type sample made of two circular discs of 75 mm diameter with the

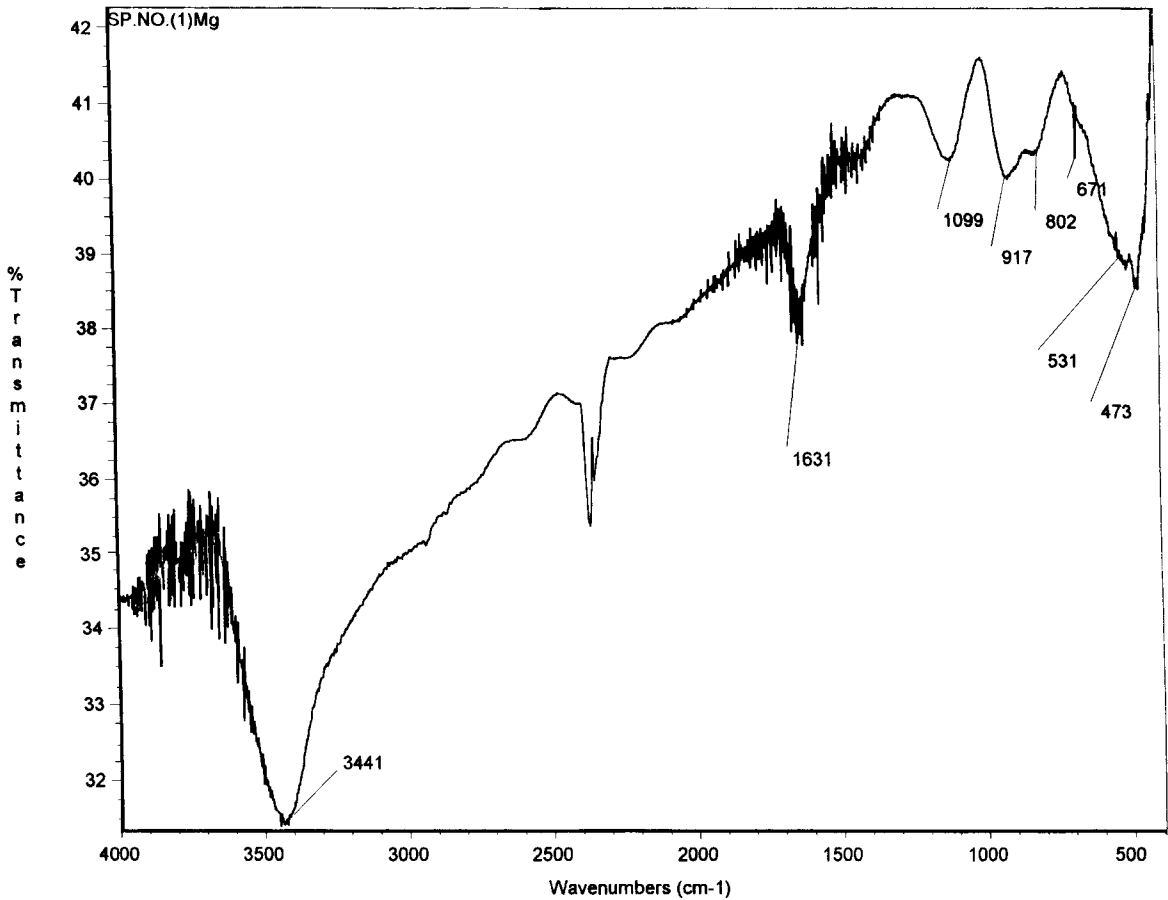


Fig. 1. Infrared spectra of anodic coating of magnesium alloy, AZ31B.

guiding grooves. Both the outside circular faces and edge of the sample were black anodized. The standard circular thermofoil heater was sandwiched between these two discs. Four copper-constantan thermocouples were mounted on the sample to monitor the sample temperature. The hemispherical emittance of black anodized samples of magnesium and magnesium–lithium alloys with temperature after error correction with reference to infrared Emissometer readings is shown in Fig. 3. The hemispherical emittance of both the coatings increases with temperature.

3.3. Thermogravimetric analysis

Figs. 4 and 5 show the TG, DTG and DSC data of black anodic oxide coatings on magnesium and

magnesium–lithium alloys, respectively. These thermoanalytical curves reveal three major changes that occur when black anodic oxide coatings are heated: (1) dehydration, (2) decomposition of chromium hydroxide and sulphate, and (3) decomposition of magnesium chromate.

3.3.1. Dehydration

Dehydration of both the anodic coatings on magnesium as well as magnesium–lithium alloys starts at $\sim 50^\circ\text{C}$ and continues until $\sim 266^\circ\text{C}$. The corresponding DTG peak of dehydration is obtained at 97°C for magnesium alloy, AZ31B. While for the coating on magnesium–lithium alloy, MLA 9, this change is represented by a dual peak at 87 and 223°C . The dehydration step in the DSC curves is represented as

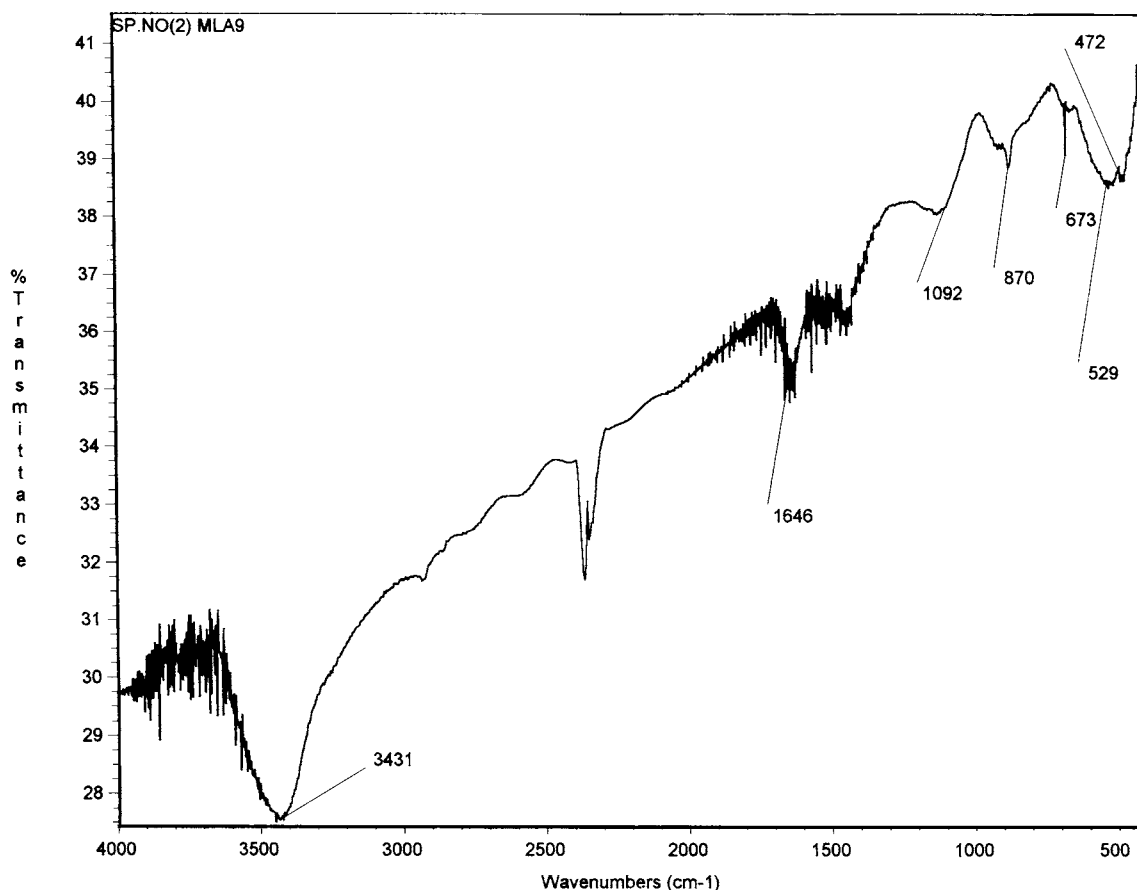


Fig. 2. Infrared spectra of anodic coating of magnesium–lithium alloy, MLA 9.

an endothermic peak [13] at 130°C for coatings on both the alloys AZ31B and on MLA 9.

3.3.2. Decomposition of chromium hydroxide and sulphate

The second stage decomposition representing the decomposition of chromium hydroxide and sulphate along with the loss of remaining water contents is observed between 266–389°C for magnesium alloy, AZ31B and 310–446°C for magnesium–lithium alloy, MLA 9. The corresponding DTG peaks are obtained at 309 and 347°C for coatings on AZ31B and MLA 9, respectively. This change is represented by DSC as an endothermic peak at around 130°C (for AZ31B) and 341°C (for MLA 9). The total weight loss in first and second stage decomposition is around 30 and 23.8% for non-heat treated and heat treated coatings, respectively

in case of magnesium alloy, AZ31B. In the case MLA 9 it is around 25.8 and 25.2% for non-heat treated and heat-treated coatings, respectively.

3.3.3. Decomposition of magnesium chromate

The third step decomposition is the decomposition of magnesium chromate to oxide. The decomposition starts around 443°C and continues up to 637°C for coatings on AZ31B. This decomposition is represented between 446 and 694°C for coatings on MLA 9. The corresponding DTG peaks are obtained at 560 and 626°C for coatings on AZ31B and MLA 9, respectively. A total mass loss of about 35.5 and 26.9% is observed up to this temperature for non-heat treated and heat-treated coatings, respectively, for coatings on AZ31B and 34.0 and 25.8% for coatings on MLA 9.

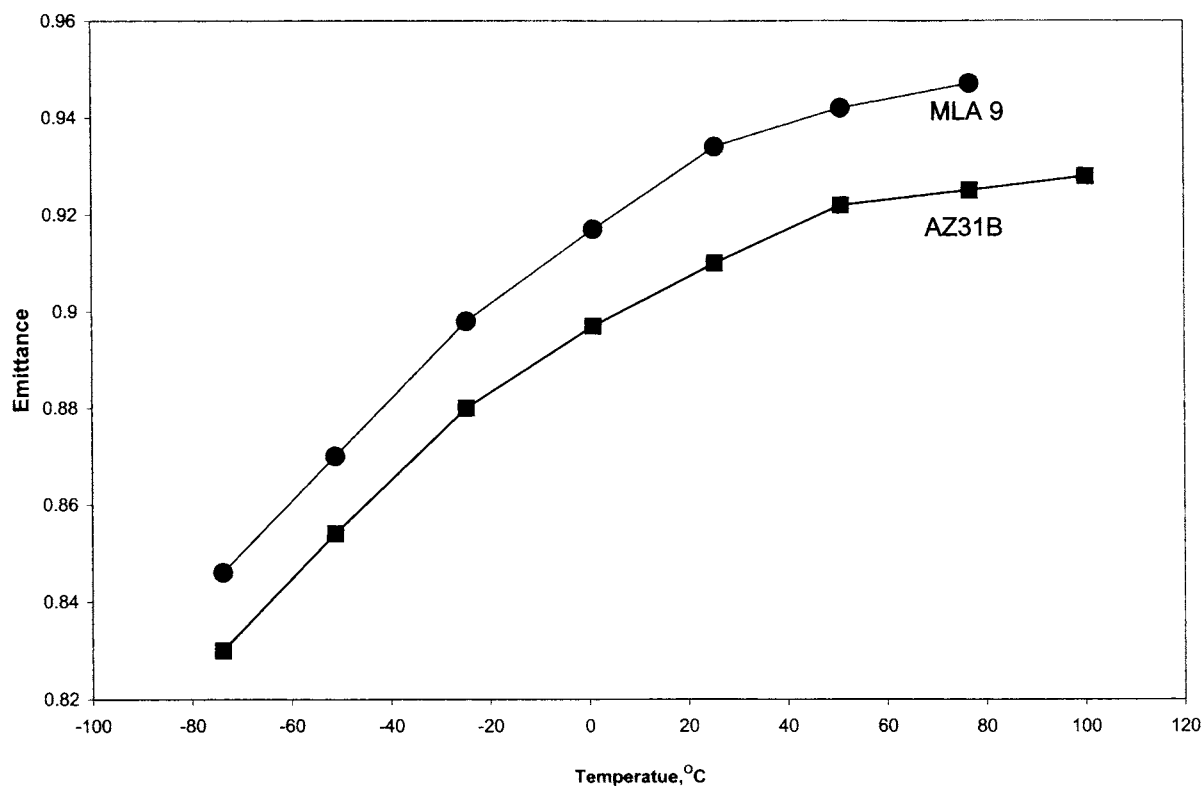


Fig. 3. Infrared emittance of anodic coating vs. temperature.

Table 1

Thermoanalytical data of anodic oxide films

Decomposition steps	Magnesium alloy, AZ31B		Magnesium–lithium alloy, MLA 9	
	Without heat treatment	Heat treated	Without heat treatment	Heat treated
1. Dehydration				
Decomposition range (°C)	50–266	50–266	50–310	50–310
Weight loss (%)	23	19	17.6	16.4
DTG, peak temp. (°C)	97	121	87	81
DSC, peak temp. (°C)	130	142	130	127
Heat of reaction (J/g)	549	263	692	639
2. Decomposition of chromium hydroxide and sulphate				
Decomposition range (°C)	266–389	266–395	310–446	310–446
Weight loss (%)	7.0	4.8	8.2	8.8
DTG, peak temp. (°C)	309	331	223, 347	223, 360
DSC, peak temp. (°C)	347	353	341	341
Heat of reaction (J/g)	265	189	770	602
3. Decomposition of magnesium chromates				
Decomposition range (°C)	443–637	466–661	446–694	446–684
Weight loss (%)	5.5	3.1	8.2	0.6
DTG, peak temp. (°C)	560	560	626	614
Total weight loss (%)	35.5	26.9	34.0	25.8

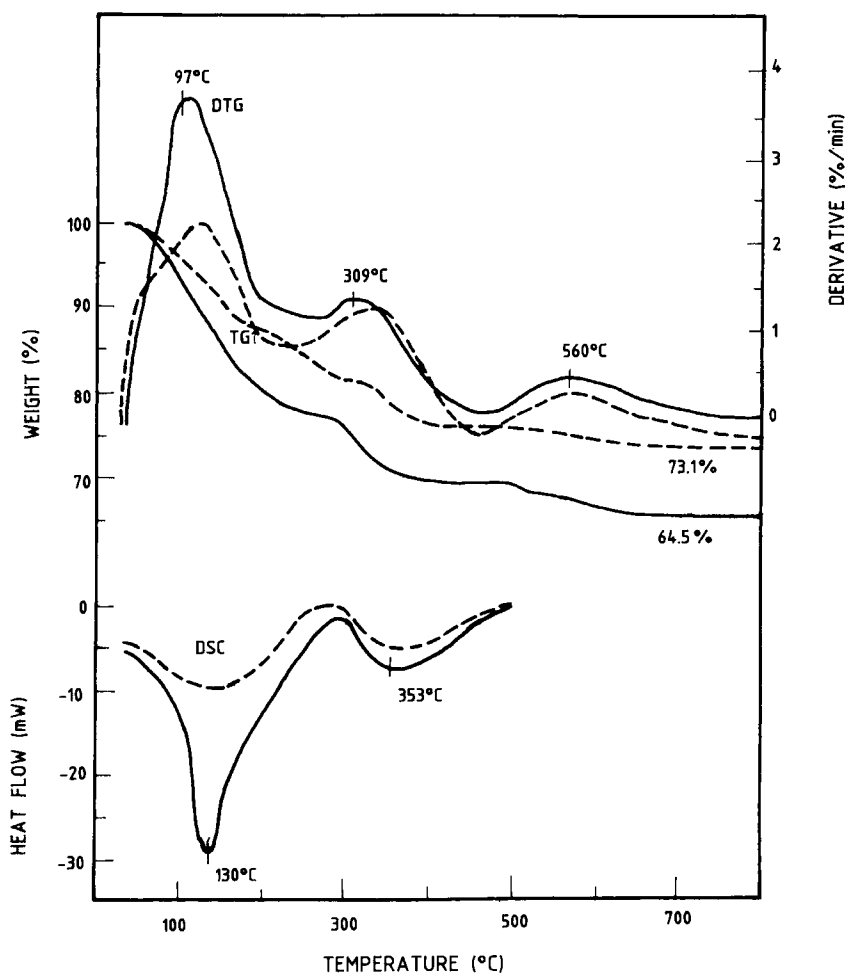


Fig. 4. Thermoanalytical curves of anodic coating of magnesium alloy, AZ31B; the dotted curves are for heat treated coatings (70°C for 2 h).

Beyond 637°C (for AZ31B) and beyond 694°C (for MLA 9) and up to 1000°C, there is no other thermal event and the coatings are thermally stable without any weight loss.

The heats of reaction for different decomposition stages of anodic film were calculated from the DSC curves using the expression $H = KA/m$, where H is the heat of reaction, K is the calibration constant, A is the area under peak and m is the mass of the sample.

At the peak temperature of 130°C, the heats of reaction for the dehydration of oxide coating on AZ31B alloy were 549 J/g for non heat treated coating and 263 J/g, for heat treated coating. While at the peak temperature of 347°C, the heats of reaction representing the decomposition of chromium hydroxide and

sulphate along with the loss of remaining water were 265 J/g for non-heat treated and 189 J/g for heat treated coatings, respectively.

For anodic coating on magnesium–lithium alloy, MLA 9, the heats of reaction at the peak temperature of 130°C (representing dehydration) were 692 J/g for non-heat treated coating and 639 J/g for heat-treated coating. While at the peak temperature of 341°C, (representing decomposition of chromium hydroxide and sulphate), the heats of reaction were 770 J/g for non-heat treated and 602 J/g for heat-treated coatings, respectively.

The thermo-analytical data of black anodic oxide coatings on magnesium alloy, AZ31B and magnesium–lithium alloy, MLA 9 is presented in Table 1.

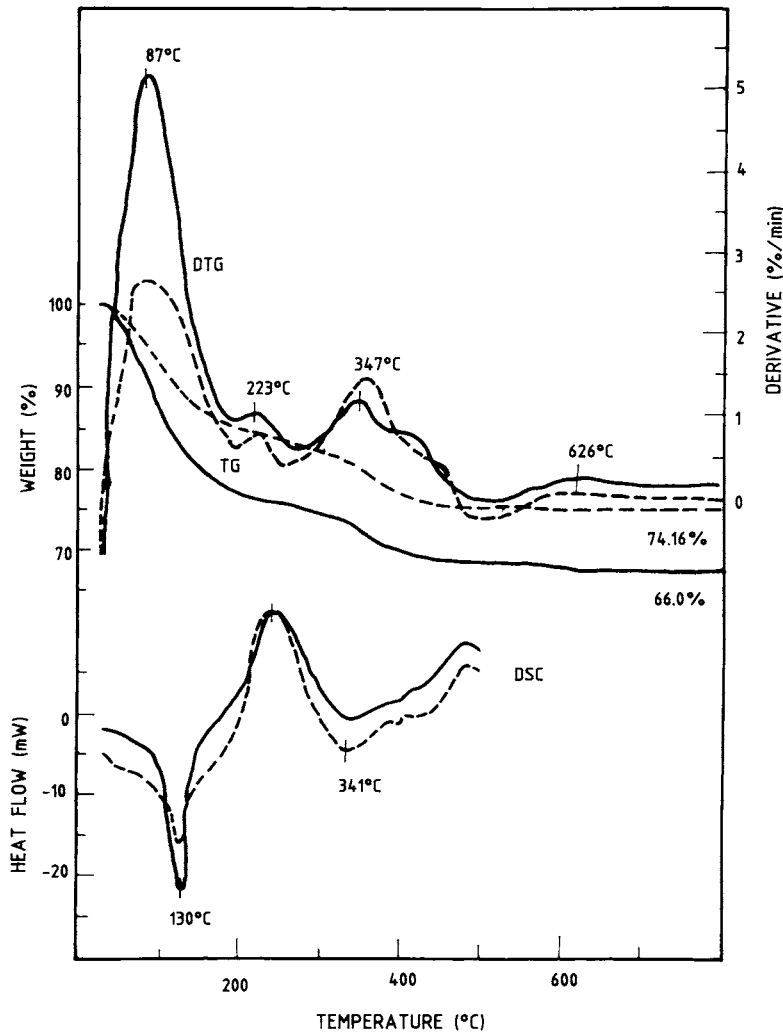


Fig. 5. Thermoanalytical curves of anodic coating of magnesium–lithium alloy, MLA 9; the dotted curves are for heat treated coatings (70°C for 2 h).

These anodic oxide coatings on magnesium are very soft (gel type) when formed. After drying and heat treatment they loose some water of hydration and attain sufficient hardness. Because of difference in the percentage of water of hydration in as anodized (non heat treated) and heat treated coatings the values of their heats of reaction are different.

The anodic oxide coatings on magnesium alloys described herein are conversion coatings. The chemical composition of coating changes as the coating thickness increases. Initially the coating has smooth fine grain morphology while at higher thickness it is

somewhat rough and powdery. The powdery coating has less percentage of water of hydration.

On magnesium alloy, AZ31B which is comparatively less prone for atmospheric corrosion, an anodic coating thickness of 5–8 μm is sufficient. While for a highly reactive magnesium–lithium alloy, MLA 9 a coating thickness of 14–18 μm is required for adequate corrosion protection. This explains the marked difference in the heats of reaction of as anodized and heat treated anodic oxide film on AZ31B alloy (less coating thickness, more difference in the percentage of water of hydration of as anodized and heat treated anodic film).

4. Conclusions

Thermal behavior of black anodic oxide coatings on magnesium alloy, AZ31B and magnesium–lithium alloy, MLA 9 has been investigated. Infrared spectral studies reveal that these coatings consist of chromium hydroxide, chromium sulphate, magnesium chromate and water of hydration.

The black anodic coatings provide high emittance (>0.80), indicating their extreme suitability for thermal control applications. Studies on measurement of hemispherical emittance of coatings verses temperature reveal that the emittance of coating increases with temperature.

Thermoanalytical studies (TG, DTG and DSC) show that the decomposition of coating proceeds through three steps, the first is dehydration, the second steps involves the decomposition of chromium hydroxide and sulphate and in the last step magnesium chromate is decomposed to oxide.

Acknowledgements

The authors are grateful to Dr. P.S. Goel, Director, ISRO Satellite Centre (ISAC), Bangalore, Mr. A.V. Patki, Deputy Director, MSA, Mr. H. Narayanamurthy,

Group Director, TSG, and Mr. H. Bhojaraj, Head, TFD, ISAC for their keen interest and encouragement. The authors duly acknowledge the support received from Mr. A. Ramasamy, V. Ramakrishnan, and N.K. Sundarasan, TTD.

References

- [1] C.R. Chakravorty, Bull. Mater. Sci. 17 (6) (1994) 733.
- [2] J. McDonald, Trans. ASM 61 (1961) 505.
- [3] J. McDonald, J. Inst. Metals 97 (1969) 353.
- [4] J. McDonald, J. Inst. Metals 99 (1971) 24.
- [5] A.K. Sharma, Trans. SAEST 30 (1) (1995) 1.
- [6] B.N. Agarwal, Design of Geosynchronous Spacecrafts, Printice-Hall, Englewood Cliffs, NJ, 1986, p. 281.
- [7] A.K. Sharma, Metal Finishing 91 (6) (1993) 57.
- [8] A.K. Sharma, R. Uma Rani, H. Bhojaraj, H. Narayanamurthy, J. Appl. Electrochem. 23 (1993) 500–507.
- [9] A. Richard Nyquist, R.O. Kagel, Infrared Spectra Of Inorganic Compounds, Vol. 4, Academic Press, New York, 1971, p. 3.
- [10] F.A. Miller, C.H. Wilkins, Anal. Chem. 24 (8) (1952) 1259.
- [11] K. Nakamoto, IR Spectra of Inorganic and Co-ordination Compounds, Wiley, New York, 1963, p. 107.
- [12] A. Ramasamy, N.K. Sundarasan, Padmanabhan, P.P. Gupta, H. Narayanamurthy, SAE Technical paper series 921329, in: Proceedings of the 22nd International Conference on Environmental Systems, Washington, July 1992.
- [13] A.K. Sharma, H. Bhojaraj, Plating Surf. Finishing 76 (2) (1989) 59–61.